

The impact of the last European deglaciation on the deep-sea turbidite systems of the Celtic-Armorican margin (Bay of Biscay)

Sébastien Zaragosi · Jean-François Bourillet ·

Frédérique Eynaud · Samuel Toucanne ·

Benjamin Denhard · Aurélie Van Toer ·

Valentine Lanfumey

Received: 21 December 2005 / Accepted: 12 September 2006 / Published online: 3 November 2006
© Springer Verlag 2006

Abstract The compilation of results obtained on three giant piston cores from the Whittard, Shamrock and Guilcher turbidite levees reveals a high-resolution stratigraphic record for the Bay of Biscay. Due to the abundance of reworked sediments in these sedimentary environments, a specific methodological approach, based on an X-ray-assisted subsampling phase associated with sedimentological, geochemical and micropalaeontological analyses, was implemented. With an accurate chronological framework, this multi-proxy investigation provides observations on the ‘Fleuve Manche’ palaeoriver and the British-Irish Ice Sheet (BIS) histories over the last 20,000 years. The results obtained highlight the direct influence of the decay of the BIS on the Bay of Biscay deep-sea clastic sedimentation during the last European deglacial phase. During this period, the annual BIS cycle of meltwater seems enough to generate seasonal turbidity

currents associated with exceptional sedimentation rates in all the Celtic and Armorican turbidite systems. With very high sedimentation rates, the turbidite levees represent the main deep-sea clastic depositional area. Long coring combined with a very careful subsampling method can provide continuous high-resolution palaeoenvironmental signals.

Introduction

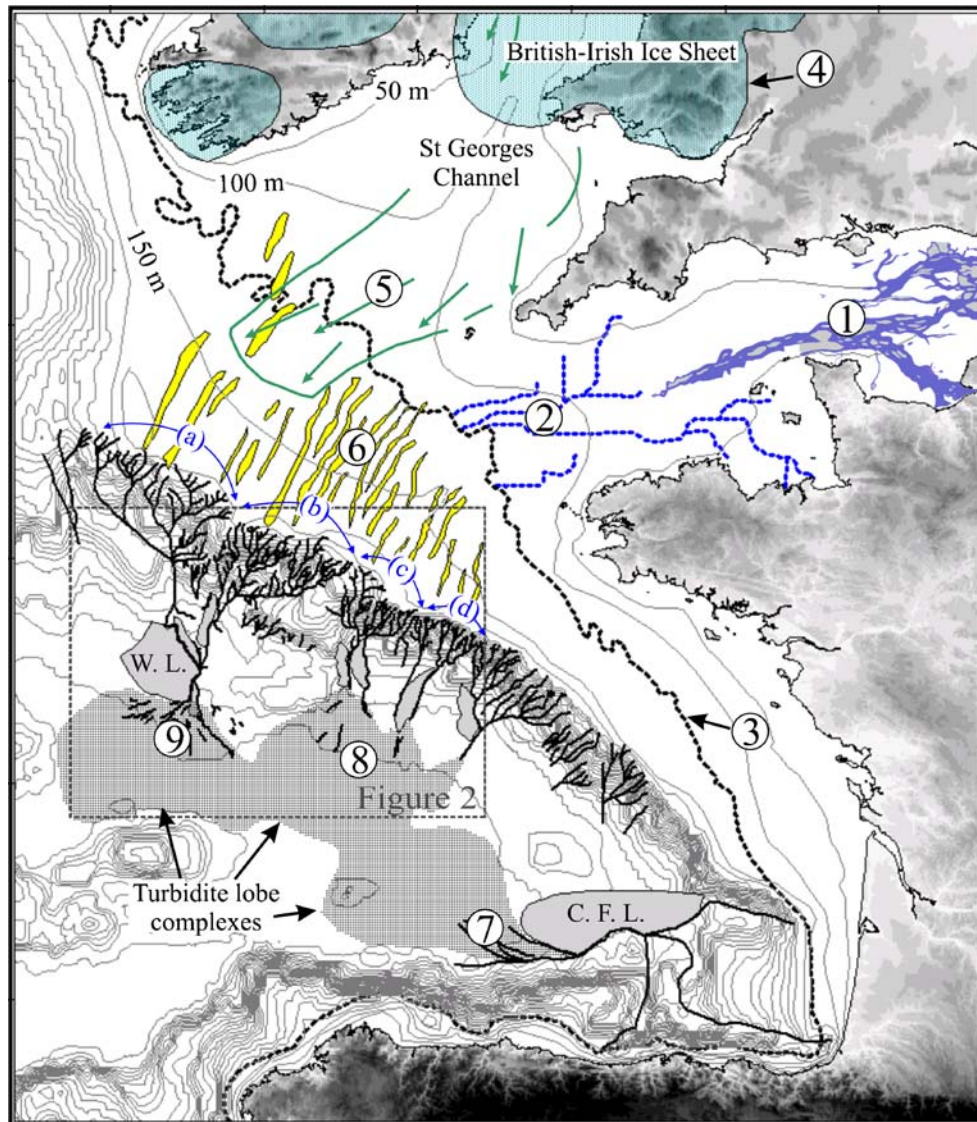
Previous studies have highlighted the fact that, during the last European deglaciation, the pronounced decay of the European Ice Sheets produced an annual cycle of meltwater and iceberg release (Mojtahid et al. 2005; Lekens et al. 2005). Associated with abrupt changes in sea-surface palaeotemperatures, these annual events produce high sedimentation rates and ‘varve-like’ layers of coarse-grained iceberg-rafted detritus (IRD) on the Meriadzek Terrace and the Trevelyan Escarpment (Figs. 1 and 2), both topographic highs of the Celtic margin (Zaragosi et al. 2001a). At the bottom of these rises, at water depths of 4,000 to 4,900 m, lie two mid-sized deep-sea clastic systems: the Celtic and Armorican turbidite systems (Droz et al. 1999; Le Suavé 2000; Auffret et al. 2000; Zaragosi et al. 2000, 2001b). These systems are fed by more than 30 incised canyons along 500 km of the Celtic and Armorican margins (Bourillet et al. 2003). These canyons, representing the major pathway for deep-sea sediment supply, have been grouped into four main submarine drainage basins (Fig. 1; Bourillet et al. 2003). Each drainage basin developed distinct, downstream submarine channels. These channels

S. Zaragosi (✉) · F. Eynaud · S. Toucanne · B. Denhard ·
A. Van Toer · V. Lanfumey
Département de Géologie et Océanographie,
Université Bordeaux I, UMR 5805 EPOC,
33405 Talence Cedex, France
e-mail: s.zaragosi@epoc.u-bordeaux1.fr

Present address:
A. Van Toer
Laboratoire des Sciences du Climat et de l’Environnement,
Avenue de la Terrasse,
91198 Gif sur Yvette Cedex, France

J.-F. Bourillet
Laboratoire Environnements Sédimentaires,
Géosciences Marines, Institut Français de Recherche pour
l’Exploitation de la Mer (IFREMER),
B.P. 70, 29280 Plouzané Cedex, France

Fig. 1 Physiography of the Celtic-Armorian margin. Bathymetric contour intervals are 50 m on the shelf (0–250 m), 500 m on the slope (500–4,000 m) and 100 m in the deep sea (4,000–4,900 m). The English channel palaeovalleys (1) and delta channels (2) are also depicted for the eastern part (Lericolais et al. 2003) and the western part of the shelf (Bourillet et al. 2003); 3 the coastline at 18,000 years ^{14}C b.p. (Bourillet et al. 2003); 4 BIS full glacial extension (Lambeck 1995); 5 ice limits and ice stream across the Celtic shelf at 21,000 years ^{14}C b.p. (McCabe and Clark 1998; Scourse et al. 2000); 6 Celtic sand banks from Reynaud et al. (1999). Canyons incising the slope are organised into drainage basins converging into feeder channels: a ‘Grande Sole’ Drainage Basin, b ‘Petite Sole’ Drainage Basin, c ‘la Chapelle’ Drainage Basin, d ‘Ouest Bretagne’ Drainage Basin (Bourillet et al. 2003). Three mid-sized turbidite systems lie at water depths of 4,000–4,900 m; 7 Cap Ferret turbidite system (Crémer et al. 1985; Faugères et al. 1998); 8 Armorican turbidite system (Le Suavé 2000; Zaragosi et al. 2001b); and 9 Celtic turbidite system (Droz et al. 1999; Auffret et al. 2000; Zaragosi et al. 2000). W. L. Whittard Levee, C. F. L. Cap Ferret Levee



are bounded by natural levees built by deposition from turbidity flows which spill out of the channels. The submarine drainage basins are (from west to east):

1. The ‘Grande Sole’ Drainage Basin (GSDB), from the Goban to Brenot spurs. The Whittard channel-levee system is located basinwards of this catchment area.
2. The ‘Petite Sole’ Drainage Basin (PSDB), from the Brenot to Berthois spurs. The Shamrock channel-levee system collects the sediment supply from this catchment area.
3. The ‘La Chapelle’ Drainage Basin (LCDB), from the Berthois to Delesse spurs. Downstream, two channel-levee systems have developed: the Blackmud and Guilcher channel-levee systems.
4. The ‘Ouest-Bretagne’ Drainage Basin, from the Delesse to Beaugé spurs, linked downstream to the Crozon channel-levee system.

These four submarine drainage basins receive the sediment supply of two distinct continental sources: (1) to the northwest, in relation with the GSDB and partly PSDB, the Irish Sea and the British-Irish Ice Sheet (BIS) which developed extensively during the two last glacial maxima (McCabe and Clark 1998; Scourse et al. 2000; Bowen et al. 2002; Mojtaid et al. 2005) and (2) to the east, in relation with the PSDB, LCDB and OBDB, the ‘Fleuve Manche’, a large palaeoriver system with a large catchment area including the continental palaeodrainage system of major West European rivers (Larsonneur et al. 1982; Gibbard 1988; Bourillet and Lericolais 2003; Lericolais et al. 2003). To study sediment fluxes from the Irish Sea and the ‘Fleuve Manche’ palaeoriver towards the deep sea, long Calypso sediment cores were collected in the Celtic and Armorican turbidite systems during the SEDICAR and ALIENOR cruises onboard the RV *Marion Dufresne II* (Bourillet and Turon 2003; Turon et al. 2004). In this paper,

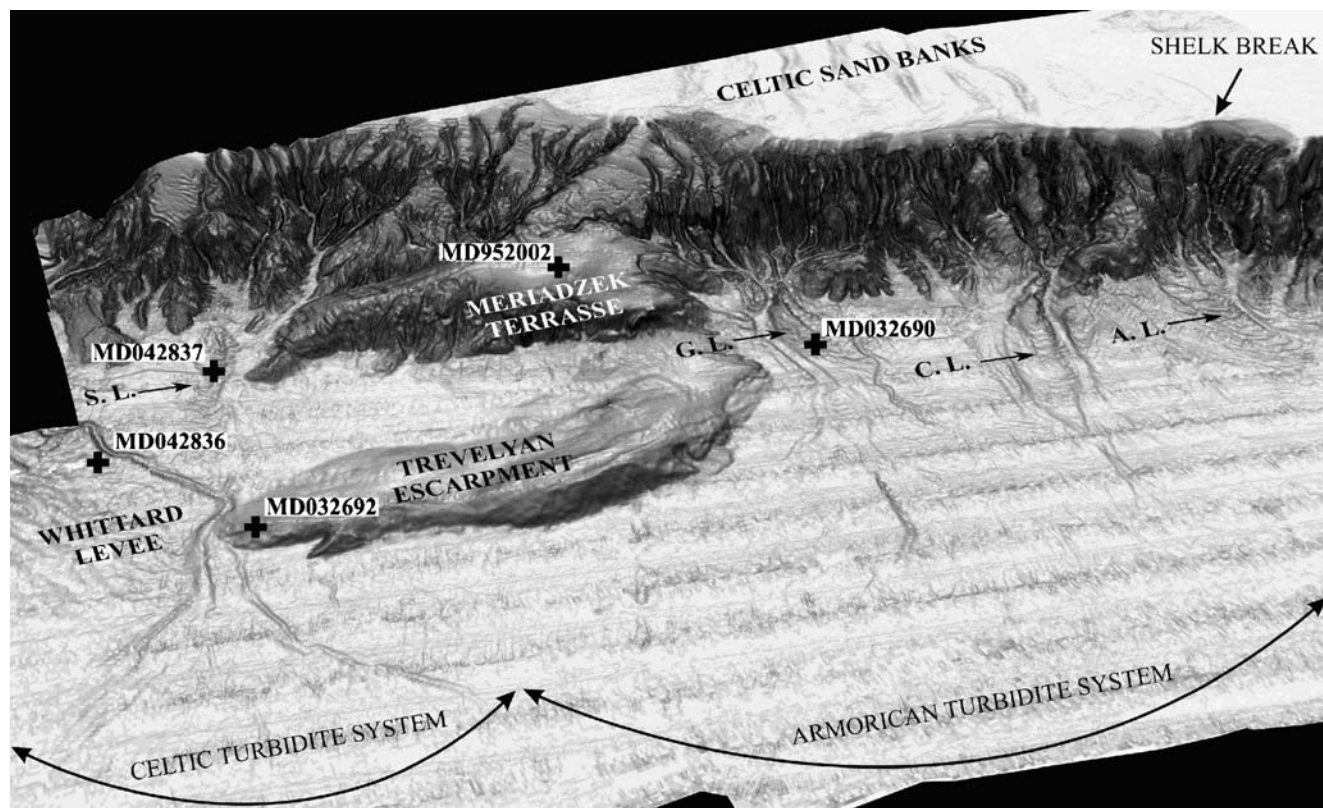


Fig. 2 Location of the studied cores with regards to the three-dimensional representation of the margin (see Fig. 1 for limits map). S. L. Shamrock Levee, G. L. Guilcher Levee, C. L. Crozon Levee, A. L. Audieme Levee. Bathymetric data are provided from the

multibeam echosounder (SIMRAD EM 12) surveys of the area conducted onboard the RV *Atalante* (IFREMER) during the cruises SEDIMANCHE (Bourillet and Loubrieu 1995), SEDIFAN I (Auffret et al. 2000) and ZEE GASCOGNE I and II (Le Suavé 2000)

results from multi-proxy analyses (i.e. physical, stratigraphical, geochemical and sedimentological) of sediment cores MD032690, MD042836 and MD042837 (Table 1), retrieved on the Guilcher, Whittard and Shamrock levees respectively, are compiled to reconstruct sedimentary processes and sediment transfers over the last 20,000 years, and to discuss the impact of the last European deglaciation on deep-sea clastic sedimentation.

Materials and methods

X-ray imagery

Thin slabs (15 mm thick) were sampled on cores MD032690, MD042836 and MD042837 at the Department

of Geology and Oceanography (Bordeaux I University) and X-ray analysed using the SCOPIX image processing tool (Migeon et al. 1999).

Major element measurements

The measurement of major elements was undertaken on core MD032690 by CORTEX X-ray-fluorescence analysis at 5-cm resolution (Jensen et al. 1998). Among the 14 major elements measured with this method, we focus on those which are significant for environmental variability, i.e. Ca, Sr and Ti.

Table 1 Core number, latitude, longitude, water depth and cruise details of the cores investigated

Core number	Latitude	Longitude	Depth (m)	Cruise	Year	Institute
MD952002	47°27.12' N	08°32.03' W	2,174	MD 105 IMAGE 1	1995	IPEV-IFREMER
MD032690	47°01.25' N	07°44.99' W	4,340	MD 133 SEDICAR	2003	IPEV-IFREMER
MD042836	47°16.57' N	10°07.69' W	4,362	MD 141 ALIENOR	2004	IPEV-IFREMER
MD042837	47°31.99' N	09°44.01' W	4,176	MD 141 ALIENOR	2004	IPEV-IFREMER

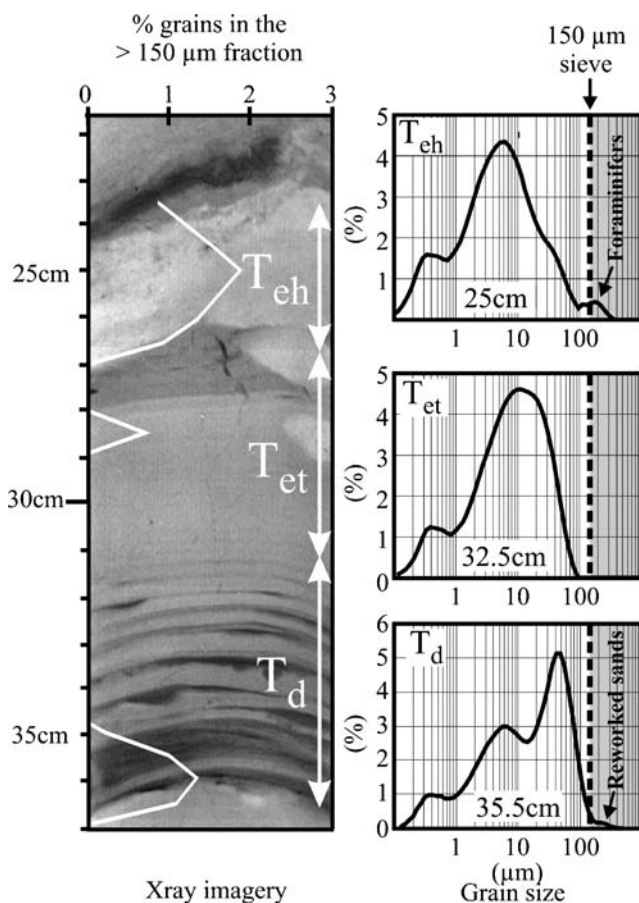


Fig. 3 X-ray imagery and Malvern grain-size measurements for a typical Whittard Levee fine-grained turbidite (Zaragosi et al. 2000). The $>150 \mu\text{m}$ residual fraction corresponds to a Malvern grain-sizer numerical sieve. The base of the sequence (T_d parts of the Bouma sequence) depicts reworked sediments in the $>150 \mu\text{m}$ residual fraction. Because of the fining-upward organisation, the $>150 \mu\text{m}$ residual fraction of the middle part of the sequence (turbiditic T_e interval of the Bouma sequence) is absent. For the top of the sequence (hemipelagic T_e interval), the positive values in the $>150 \mu\text{m}$ residual fraction are related to autochthonous planktonic Foraminifera. Thus, for stratigraphic investigation, it is necessary to take subsamples only in the hemipelagic T_e interval. However, the lack of reworked sediments in the $>150 \mu\text{m}$ residual fraction of the turbiditic T_e implies a comfortable margin of error during sampling

Foraminifera-stratigraphy

To establish foraminifer stratigraphy, reworked sediments need to be avoided. On turbidite levees, however, turbidites are the most volumetrically significant facies. Therefore, the abundance of reworked sediments makes the subsampling phase delicate. Turbidite overflow sequences present a general thinning- and fining-upward trend, from very fine turbiditic sand (T_d division of the Bouma turbidite sequence; Bouma 1962) to turbidite and hemipelagic clay intervals (T_e and T_{eh} divisions). In order to exclude reworked sediments in the $>150 \mu\text{m}$ fraction, X-ray imagery was used to assure sampling in

the hemipelagic clay intervals located between the turbidite sequences (Fig. 3). The subsamples were sieved through a $150 \mu\text{m}$ mesh. The residual fraction comprises primarily biogenic benthic and planktonic foraminifers and coarse terrigenous detrital grains (potentially ice rafted detritus).

Qualitative and quantitative analyses of planktonic Foraminifera were performed on the $>150 \mu\text{m}$ fraction. Counting focused on the species *Neogloboquadrina pachyderma* sinistral, a morphotype which today dominates the North Atlantic polar environments. The stratigraphical framework of the cores is based on the combination of the *N. pachyderma* s. percentage curve and AMS ^{14}C dating (Table 2).

To obtain a precise age model, the *N. pachyderma* s. percentage curve acquired on the proximal core MD952002 (Fig. 2; Zaragosi et al. 2001a) is compared with the percentage curve of the same species obtained on the studied cores. These different curves display a clear similarity (Fig. 4). The age scale of core MD952002 was previously well constrained (19^{14}C AMS dates between 0 and 30 ka; Table 2; Groussset et al. 2000; Zaragosi et al. 2001a).

Terrigenous characterization

The coarse detrital grains were characterized and counted in all samples on the same fractions as those used for the microfauna analyses. These grains include all the lithic grains coarser than $150 \mu\text{m}$ and contain IRD, which indicates iceberg melt fluxes.

Subsamples on bulk sediments were taken for measurements of carbonate content using gasometric calcimetry, and grain-size measurements using a Malvern MASTER SIZER S.

Thin sections

To obtain high-resolution sedimentological information, a modified impregnation protocol was adapted, for wet fine-grained sediments, from the method described by Bénard (1996). Fresh cores were sampled with oriented perforated aluminium boxes ($100 \times 45 \times 13 \text{ mm}$). The samples were subsequently dehydrated with a graded series of acetone-water solutions (25, 50, 75 and 100%). The acetone was fully dried using a molecular sieve (4A pellets) under closed circuit with a peristaltic pump enabling continuous acetone circulation. After the acetone change, the subsamples were placed in plastic boxes with impregnating solution. This solution consists of Crystic 17449 resin, acetone and catalyst (Butanox M50), at ratios of

Table 2 AMS ^{14}C ages with calendar correspondences (Bard 1998)

Core number	Depth (cm)	Conventional age b.p. (reservoir correction) (years)	Calendar age cal. b.p. (years)	Species analysed	Origin
MD95-2002	0	1,660±70	1,624	<i>G. bulloides</i>	LSCE-99360
MD95-2002	140	9,080±90	10,329	<i>G. bulloides</i>	LSCE-99361
MD95-2002	240	10,790±100	12,809	<i>N. pachyderma</i> s.	LSCE-99362
MD95-2002	420	13,330±130	15,798	<i>N. pachyderma</i> s.	LSCE-99363
MD95-2002	454	13,800±110	16,426	<i>N. pachyderma</i> s.	LSCE-99364
MD95-2002	463	14,020±120	16,709	<i>N. pachyderma</i> s.	LSCE-99365
MD95-2002	510	14,170±130	16,897	<i>N. pachyderma</i> s.	LSCE-99366
MD95-2002	550	14,430±70	17,327	<i>N. pachyderma</i> s.	Artemis-003242
MD95-2002	869	14,900±70	18,241	<i>N. pachyderma</i> s.	Artemis-003243
MD95-2002	875	14,880±160	18,224	<i>N. pachyderma</i> s.	Artemis-003244
MD95-2002	1,320	18,450±90	22,062	<i>G. bulloides</i>	Artemis-003245
MD95-2002	1,340	19,030±100	22,514	<i>G. bulloides</i>	Artemis-003246
MD95-2002	1,390	20,220±80	24,690	<i>G. bulloides</i>	Artemis-003247
MD95-2002	1,424	19,840±60	23,777	<i>N. pachyderma</i> s.	Beta-123696
MD95-2002	1,453	20,030±80	23,984	<i>N. pachyderma</i> s.	Beta-123698
MD95-2002	1,464	20,200±80	24,174	<i>N. pachyderma</i> s.	Beta-123699
MD95-2002	1,534	21,850±70	25,734	<i>N. pachyderma</i> s.	Beta-123697
MD95-2002	1,610	24,010±250	28,222	<i>N. pachyderma</i> s.	Beta-99367
MD95-2002	1,664	25,420±230	29,830	<i>N. pachyderma</i> s.	Beta-99368
MD03-2690	151	8,730±60	9,722	<i>G. bulloides</i>	Artemis-001894
MD03-2690	245	9,450±60	10,603	<i>G. bulloides</i>	Artemis-003233
MD03-2690	626	12,620±60	14,790	<i>G. bulloides</i>	Artemis-003234
MD03-2690	692	12,770±70	14,972	<i>N. pachyderma</i> s.	Artemis-003235
MD03-2690	1,094	13,840±70	16,266	<i>N. pachyderma</i> s.	Artemis-003236
MD03-2690	1,213	14,030±70	16,495	<i>N. pachyderma</i> s.	Artemis-003237
MD03-2690	1,885	14,650±70	17,241	<i>N. pachyderma</i> s.	Artemis-003238
MD03-2690	2,233	14,960±70	17,613	<i>N. pachyderma</i> s.	Artemis-003239
MD03-2690	2,276	15,080±70	17,760	<i>N. pachyderma</i> s.	Poznań Radiocarb. Lab.
MD03-2690	3,156	18,850±100	22,234	<i>G. bulloides</i>	Artemis-003240
MD03-2690	3,376	20,560±70	24,236	<i>N. pachyderma</i> s.	Artemis-003241
MD03-2690	3,576	21,880±120	25,770	<i>N. pachyderma</i> s.	Poznań Radiocarb. Lab.

100:15:0.85 per volume. Fluorescent dye (UVITEX OB at 0.73 g/l) was dissolved in the mixture to enable subsequent fluorescent light analysis. The plastic boxes were then placed in a desiccator at a pressure of 0.6 bar for 2 days. Samples were removed from the desiccator and left to polymerize for 4 weeks at room temperature, and finally under sunlight for 4 weeks to harden.

Vertical cross-sections were made in the middle of the sediment/resin samples using a diamond saw. One side of each block was polished using a rotating lapidary unit with silicon carbide polisher (F320 and F500). The clean surfaces obtained were attached to 12×4.5 cm microscope slides using Crystic resin, Butanox catalyst and hardening agent (Kovi NL-51P accelerator). The bonded blocks were cut to approximately 100 µm using a precision saw (ESCIL LT-260) and thereafter hand polished to a thickness of 30 µm using the rotating lapidary unit. Finally, cover slips were fixed on the thin sections using the collage resin mixture.

Thin-section images were acquired using a fully automated Leica DM6000 B Digital Microscope with multiple magnifications. Illumination in the ultraviolet band also enables fluorescence imaging.

Results

Stratigraphy and sedimentation rates

Figure 4 presents the *N. pachyderma* s. percentages of the studied cores. The main reworked sedimentary composition of turbidite levees can make it difficult to generate accurate stratigraphic curves. The subsampling procedure (cf. Materials and methods; Fig. 3) used here to extract the hemipelagic signal enables the recovery of the hemipelagic layers, avoiding the turbidite laminae. Therefore, the main palaeoclimatic events of the marine isotopic stages (MIS) 1 and 2 are distinctly recorded (i.e. the Holocene, Younger

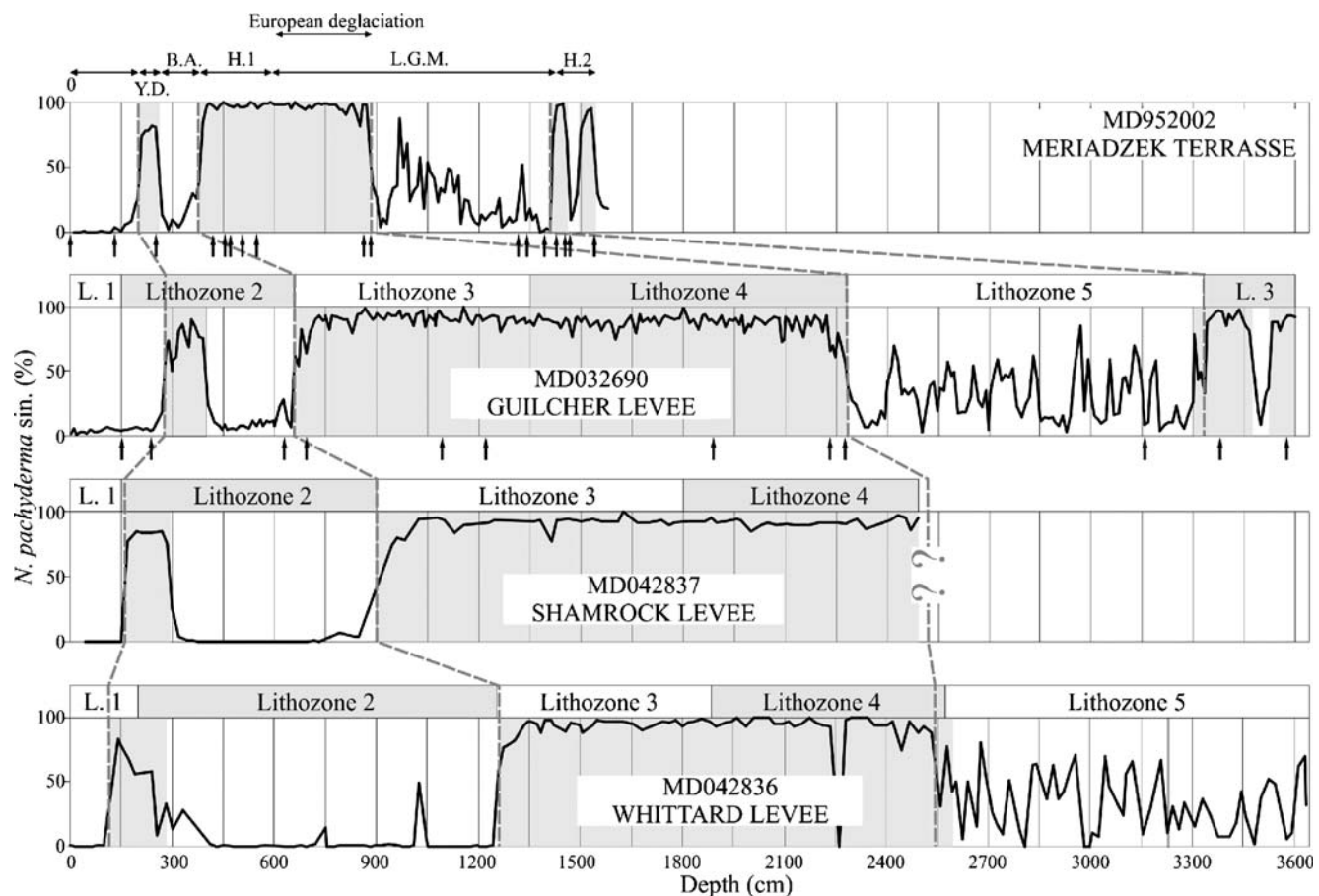


Fig. 4 Compilation of the foraminifer *N. pachyderma* s. (%) abundance and lithozone organisation for cores MD952002, MD032690, MD042837 and MD042836. Arrows indicate AMS ^{14}C dating (Table 2)

Dryas, Bølling-Allerød, Heinrich events H1 and H2, and the last European deglaciation phase).

Previously, the MD952002 core, located on the Meriadzek Terrasse, was the sedimentary record with the highest sedimentation rates known in the Bay of Biscay (Zaragosi et al. 2001a). Cores MD032690, MD042836 and MD042837 present rates two to three times higher during the last 20,000 years.

XRF results

Sr (alkaline earth element) is fixed by calcifying organisms at the same time as Ca. For this reason, Sr is used in marine environments as a marker of strictly biogenic origin (Martin et al. 2004). Conversely, Ca can be supplied from terrigenous sources (including feldspars and clays). In the MD032690 core, Ca is mainly sourced from biogenic CaCO_3 , as suggested by the covariation of the Ca and Sr data (Fig. 5).

Ti is a common constituent of rocks such as gneisses or schists and therefore primarily indicates a terrigenous continental source. The Ti/Sr ratio is used to discern terrigenous versus biogenic supplies. The Ti/Sr ratio shows

elevated values during the last glacial stage and during the Younger Dryas. The Bølling-Allerød and Holocene period are characterized by a low Ti/Sr ratio (<5). During the last glacial stage, Ti/Sr evolution is positively related to the number of sediment laminae (Fig. 5), i.e. a high amount of laminae is synchronous with high Ti/Sr ratio values. The highest Ti/Sr ratios and occurrence of laminae are observed during the European deglaciation event (between 13,870 and 15,060 years ^{14}C b.p.).

Lithology

Cores MD032690, MD042836 and MD042837 were subdivided into five lithozones (Fig. 4). These lithozones were defined using photography, X-ray imagery, grain-size measurements, CaCO_3 content, XRF measurements and thin-section analysis (cf. Figs. 6, 7 and 8).

Lithozone 1: homogenous structureless marly ooze

Lithozone 1, observed in the upper part of the studied cores, presents high CaCO_3 contents (30–60%) and very low Ti/Sr

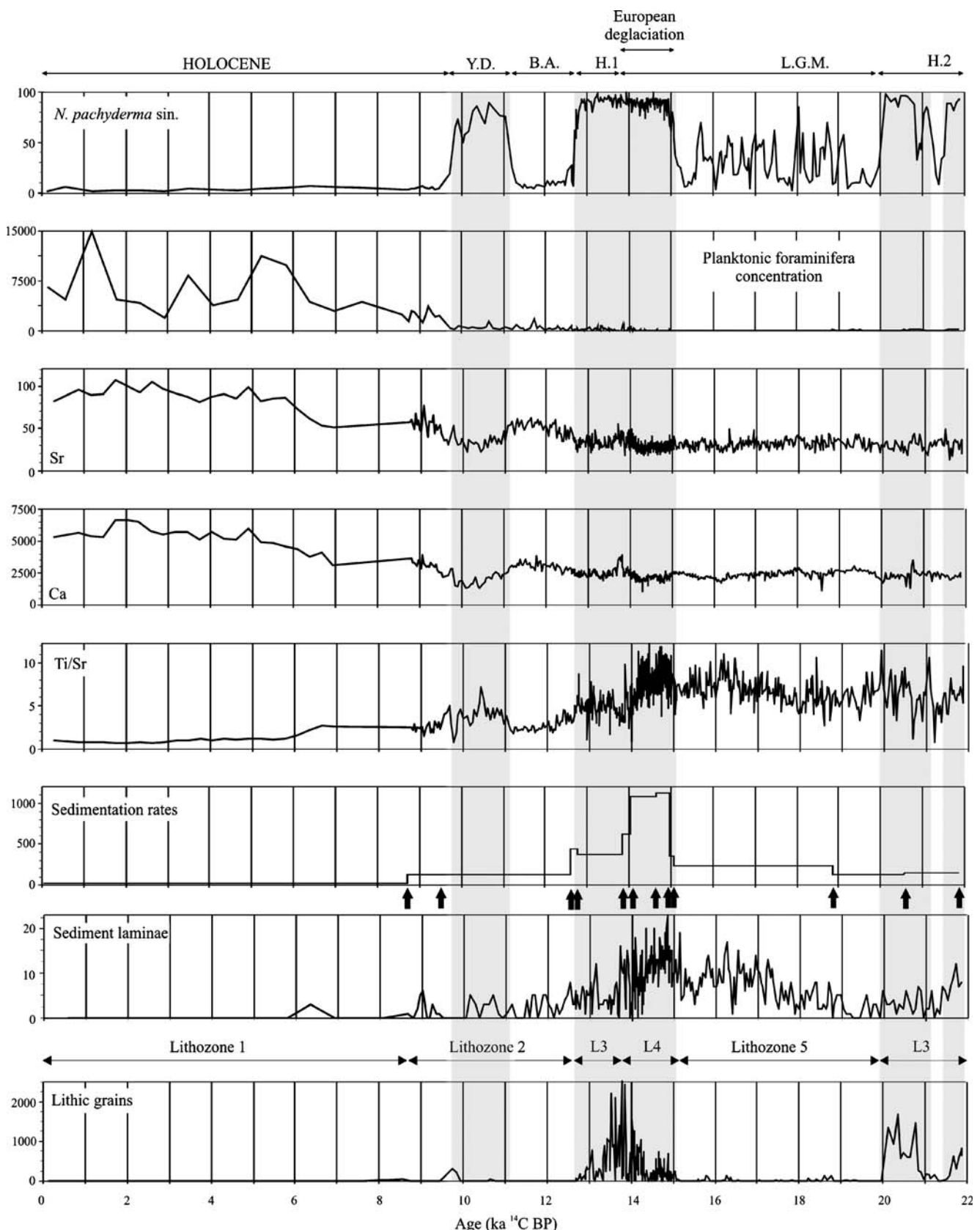


Fig. 5 Timescale of core MD032690 (Guilcher Levee): abundance of the foraminifer *N. pachyderma s.* (%), planktonic foraminifer contents (number/g), Ca and Sr records obtained by XRF (cps), Ti/Sr ratio obtained by XRF, sedimentation rates (cm/1,000 years), frequency of sediment laminae (number/10 cm), abundance of coarse ($>150 \mu\text{m}$) lithic grains (grain/g). Arrows indicate AMS ^{14}C dating (Table 2). Highlighted intervals mark polar sea-surface conditions

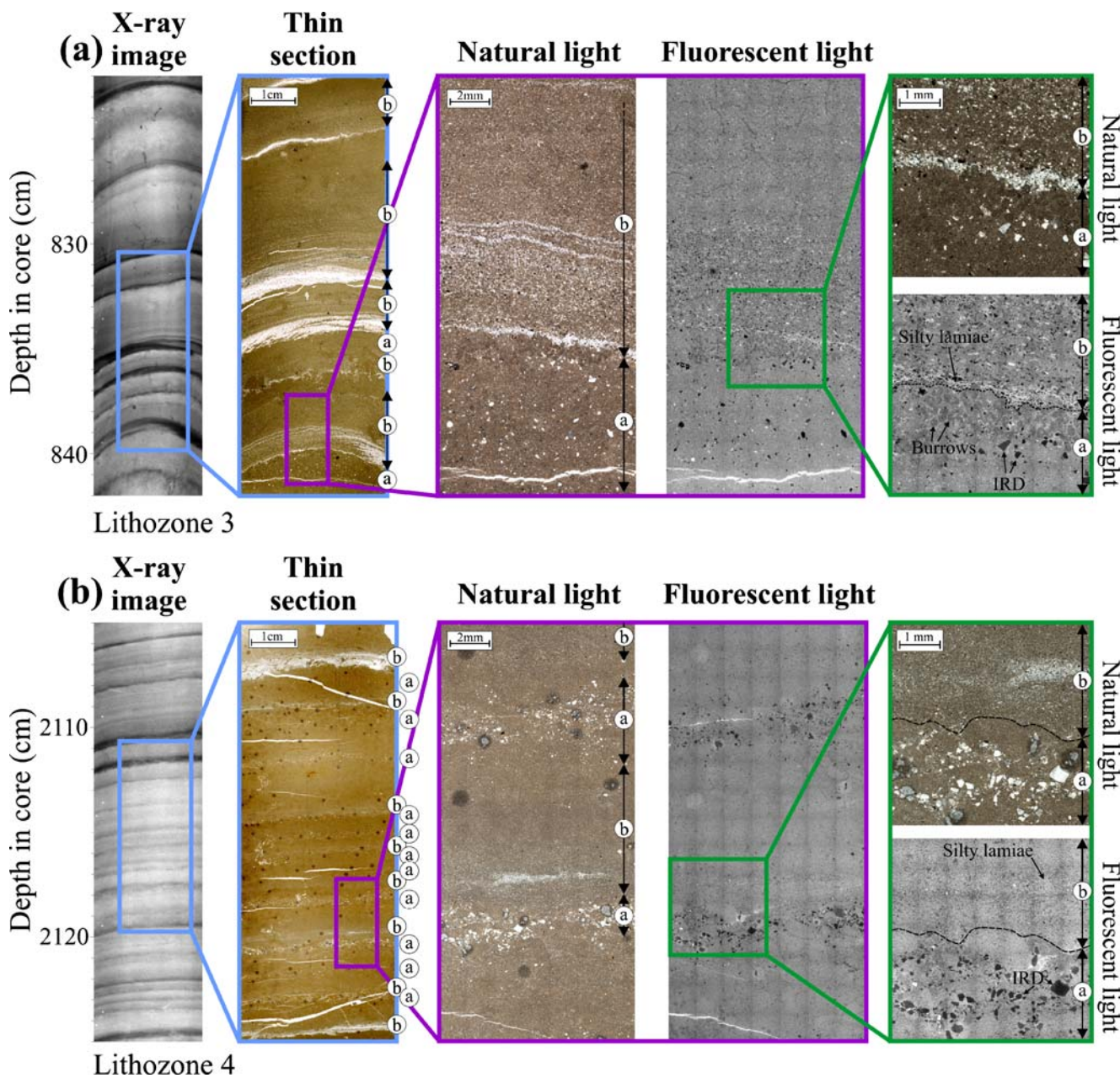


Fig. 6 Variable-scale X-ray imagery and sediment thin-section microphotography of MD03690 lithozones 3 and 4: **a** IRD-rich clay layer, **b** fine-grained turbidite

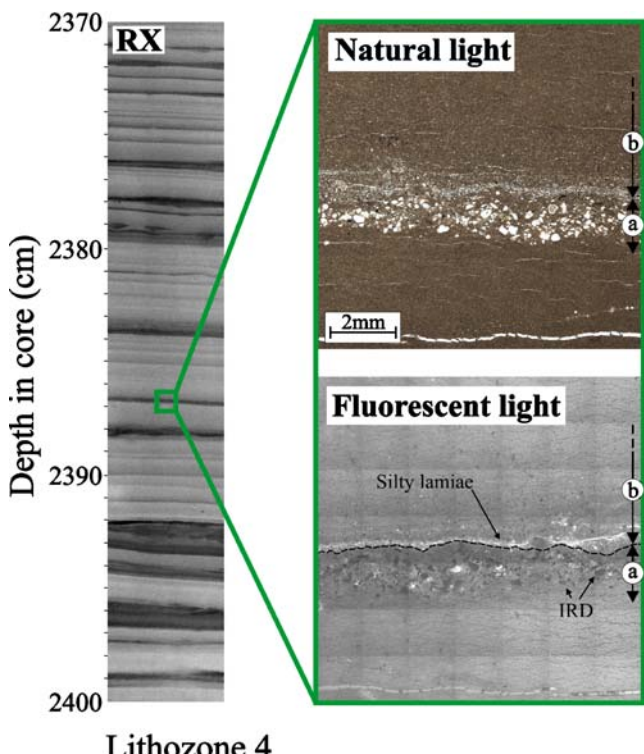
ratios. These sediments of homogenous appearance are characterized by an absence of lithic grains in the >150 µm fraction and are associated with low sedimentation rates (about 18 cm/1,000 years).

The content of *N. pachyderma* s. is always lower than 8% and the amount of planktonic foraminifers shows enhanced values of between 2,000 and 15,000 foraminifers per gram.

This lithozone, forming the modern deep-sea Bay of Biscay seafloor, has been interpreted on the Whittard, Shamrock and Guilcher turbidite levees as pelagic to hemipelagic drape deposits without significant terrigenous supplies from the shelf.

Lithozone 2: homogenous structureless clay with rare fine-bedded very fine sand, silt and clay sequences

Lithozone 2, observed during the Bølling-Allerød, Younger Dryas and Early Holocene, is characterized by intervals of homogenous structureless clay interbedded with centimetric fine-grained turbidites. CaCO₃ content is lower than 30%. The Ti/Sr ratio presents intermediate values, except for higher values during the Younger Dryas. These higher values are linked to the cold sea-surface conditions of this event, with low biogenic production. The content of *N.*



Lithozone 4

Fig. 7 X-ray imagery and sediment thin-section microphotography of MD042836 lithozones 4: **a** IRD-rich clay layer, **b** fine-grained turbidite

pachyderma s. presents values below 8% except during the Younger Dryas cold event, and the amount of planktonic

foraminifers per gram ranges between 300 during the Bølling-Allerød and 4,000 during the Early Holocene.

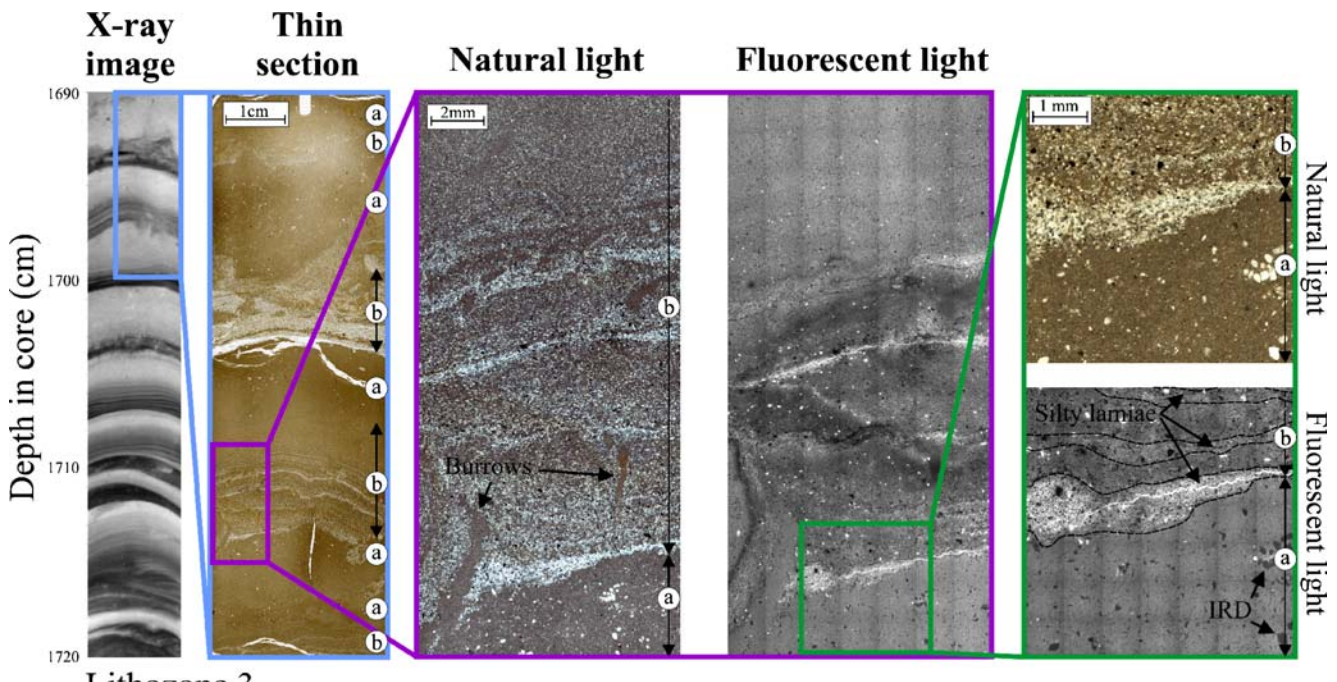
For core MD032690, the sedimentation rate decreases from high values during the Bølling-Allerød (176 cm/1,000 years) to low values (18 cm/1,000 years) for the Early Holocene.

Lithozone 2 is interpreted as hemipelagic deposits with episodic fine-grained turbidite supply.

Lithozone 3: laminated, very fine sand, silts, clay and IRD-rich layers

Sediments of lithozone 3 contain frequent sequences of thinning- and fining-upward, very fine sand and silt laminae with sharp basal contacts. Sometimes cross-stratifications (Figs. 6 and 8) and IRD-rich millimetric clay layers are observed. The sequences of very fine sand and silt laminae are interpreted as fine-grained turbidites. Turbidite layers are thin (2–10 cm) and the layers rich in ice-raftered debris are often located immediately below the fine-grained turbidites.

Sediments in lithozone 3 show low CaCO_3 contents (13–30%) and an intermediate Ti/Sr ratio. Lithozone 3 is synchronous with Heinrich events H1 (12,700–14,300 years ^{14}C b.p.; Zaragosi et al. 2001a) and H2 (19,700–22,300 years ^{14}C b.p.; Zaragosi et al. 2001a), and presents very high values in the >150 μm lithic grain fraction as well as high sedimentation rates in core MD032690 during the Heinrich 1 event (about 375 cm/1,000 years). The *N. pachyderma* s. monospecific assemblage (~100%) indicates



Lithozone 3

Fig. 8 Variable-scale X-ray imagery and sediment thin-section microphotography of MD042837 lithozones 3: **a** IRD-rich clay layer, **b** fine-grained turbidite

polar sea-surface conditions, and the amount of planktonic Foraminifera ranges between 100 and 800 foraminifers per gram.

Lithozone 3 reveals significant turbidite supply from the shelf associated with frequent ice-raftering events.

Lithozone 4: very fine-bedded silt, clays and IRD-rich clay layers

Lithozone 4 presents a similar combination of turbidite and ice-raftering sequences to lithozone 3. Compared to lithozone 3, the thickness of fine-grained turbidite layers is low and the frequency of the IRD-rich laminae is high. Turbidites are very thin (about 1 cm) and IRD layers are almost always located at the base and top of the fine-grained turbidites (Figs. 6 and 7). For core MD032690, the sedimentation rate is extremely high (about 1,123 cm/1,000 years).

Sediments of lithozone 4 present low CaCO_3 contents (13–19%) and high Ti/Sr ratios. The *N. pachyderma* s. monospecific assemblage (~100%) indicates polar sea-surface conditions. The amount of planktonic Foraminifera ranges between 10 and 200 foraminifers per gram.

Lithozone 4, synchronous with the European deglaciation event (14,300–15,000 years ^{14}C b.p.; Zaragosi et al. 2001a; Mojtabah et al. 2005), reveals extremely important turbidite supply from the shelf associated with frequent ice-raftering events.

Lithozone 5: fine-bedded very fine sands, silt and clays

Sediments of lithozone 5 contain frequent sequences of thinning- and fining-upward very fine sand and silt laminae interpreted as fine-grained turbidites. Lithozone 5, with low CaCO_3 contents (13–24%), presents an intermediate Ti/Sr ratio and a very low foraminifer content (<50 foraminifers per gram).

Lithozone 5, observed on the Whittard and Guilcher levees during the main part of the Last Glacial Maximum (LGM, 21,000 to 15,000 years ^{14}C b.p.), presents sedimentation rates of about 175–250 cm/1,000 years. The high variability of the *N. pachyderma* s. percentages (2–85%) indicates high climatic variability during the LGM.

Discussion

Channel-levee morphology

The Celtic and Armorican margin deep-sea environments include channels located southwards of the drainage basins showing two morphological types: (1) straight and relatively large (Shamrock, Brest and Crozon channels) and (2)

sinuous (Whittard and Guilcher channels). All these channels have developed strongly asymmetrical bordering levees. The straight channels are 1,000–5,000 m wide, 50–80 km long and edged by 50–260 m high right levees. The sinuous channels are 1,500–2,500 m wide, 60–100 km long and edged by 70–270 m high right levees. The size of most of the levees is relatively constant (800–500 km²), except for the oversized Whittard Levee which spread over more than 3,500 km².

The comparison between the size of the levees and sedimentation rates of the studied cores reveals no relationship between levee development and Late Quaternary accumulation rates. Indeed, mean sedimentation rates in cores MD032690 (Guilcher Levee) and MD042836 (Whittard Levee) are comparable, despite the surface area of the Whittard Levee being seven times greater. Sediment composition is also similar for each levee, as shown by the uniform lithozone organisation (Fig. 4). Previous study of several submarine channel levees (Skene et al. 2002) demonstrates a distinct relationship between levee architecture and channel dimension. Despite this relationship, no systematic variation between the Whittard, Shamrock and Guilcher levee sizes and sedimentation rates or sediment type is seen. Consequently, the possibility of allocyclic processes such as sediment source and sedimentary process variability cannot explain the larger development of the Whittard Levee. Autocyclic processes such as low avulsion rates and high levee stability seem more appropriate in explaining this greater size.

Evolution of sedimentary processes

The development of the Celtic and Armorican turbidite systems began during the Miocene (Droz et al. 1999). Core control in this study enables the reconstruction of the sedimentary history during the MIS 1 and 2 (0–22,000 years ^{14}C b.p.) only. During this period, these systems do not appear to have been built-up with a gradual or constant sediment supply. The five observed lithozones indicate distinct episodes of growth characterized by several depositional processes.

It is expected that cores collected on turbidite levees record autocyclic processes related to the overall increase in channel relief through time (Manley et al. 1997). These autocyclic processes involve a fining- and thinning-upward trend of the overflow sequences. However, on the Guilcher, Shamrock and Whittard levees during the last 15,000 years ^{14}C b.p., the lithozone organisation depicts an opposite trend. Indeed, the transitions between lithozones 4, 3 and 2 are characterized by a thickening-upward evolution of the turbidite sequences. The synchronous evolution on the whole margin therefore appears to be linked to allocyclic

processes. These processes can be linked to the evolution of sediment supply from the ‘Fleuve Manche’ palaeoriver and the BIS, as well as continent-deep ocean connection quality linked to sea-level rise.

The stratigraphic framework established for the Guilcher, Shamrock and Whittard levees reveals synchronicity for the five characteristic lithozones (Fig. 4). Sediments deposited on the levees during the main part of the LGM (21,000 to 15,000 years ^{14}C b.p.) are characterized by frequent fine-grained turbidites (lithozone 5) and relatively high sedimentation rates. The sea-level lowstand associated with high fluvial flux related to heat and moisture supplies linked to the North Atlantic Drift (Zaragosi et al. 2001a) seems to explain the observed high sedimentation rates. In this configuration, a wide spectrum of material was available to be transported to the deep sea. This high sediment supply from the shelf was also contemporaneous with the existence of the Irish Sea ice stream, the main drainage conduit for the BIS (Scourse et al. 2000; Richter et al. 2001). During the LGM, this ice stream, located in the vicinity of the St. Georges’ Channel (Fig. 1), flowed southwards towards the Armorican and Celtic turbidite systems.

At 15,000 years ^{14}C b.p., a major change in deposition pattern occurred on all turbidite levees. This change is characterized by the occurrence of ice-raftered deposits as well as by a significant increase in sedimentation rates and Ti/Sr ratios (lithozone 4). These changes, synchronous with the last European deglaciation event (Zaragosi et al. 2001a), indicate increased continental sediment supply associated with frequent deposition of ice-raftered debris. Between

15,000 and 14,200 years ^{14}C b.p., similar ice-raftered deposits occur on the Trevelyan Escarpment and Meriadzek Terrace (Zaragosi et al. 2001a; Mojtaid et al. 2005), two tectonic topographic highs located in the same area (Fig. 2). These deposits have been interpreted as annual marine ‘varves’ related to the annual cycle of meltwater and iceberg release from the disintegrating BIS.

Thin sections of sediments of the deglaciation phase (Figs. 6 and 7) reveal the link between turbidite and IRD-rich layers. Based on sedimentation rates of about 1,123 cm/1,000 years, the thin section in Fig. 6 (core MD032690, Guilcher Levee) represents about 8.5 years of sedimentation. In all, 11 ice-raftered laminae and eight fine-grained turbidites are found. Each of the six central turbidites is bordered at the base and the top by IRD-rich laminae. Sharp basal contact and gradual upper top contact indicate that, in fact, each IRD layer, related to the same seasonal iceberg release, is subdivided into two by a turbidite unit (Fig. 9). Thus, during the European deglaciation phase, the annual cycle of meltwater from the disintegrating BIS appears enough to have generated seasonal turbidite flows in the whole of the Celtic and Armorican turbidite system catchment areas through all the canyons of the ‘Grande Sole’, ‘Petite Sole’ and ‘La Chapelle’ drainage basins.

During this period, the connection between the two potential continental sedimentary sources (i.e. the ‘Fleuve Manche’ palaeoriver and the Irish Sea glacial systems) and the canyons must have been efficient. Indeed, the synchronicity between the turbidite flows and iceberg release indicates a very short sedimentary transit on the shelf. The significant increase of the sedimentation rates associated with the high Ti/Sr ratios also attests to an intensification of terrigenous transfer during this period.

Around 14,000 years ^{14}C b.p., immediately before the Heinrich 1, a new synchronous change occurs in all studied turbidite levees. This change results in an increase in the thickness of the fine-grained turbidite sequence, in a decrease in the number of ice-raftered layers and in decreases in sedimentation rates and Ti/Sr ratios (lithozone 3). The relationship between the ice-raftered layers and the fine-grained turbidites is no longer systematic, and the fine-grained turbidites are thicker but less frequent. This evolution would represent the beginning of deterioration in the connection efficiency between the fluvial continental systems and the canyon heads in relation to synchronous sea-level rise.

During the Bølling-Allerød, the ice-raftered deposits definitively disappear and the sedimentation rates decrease strongly (lithozone 2). This drop, associated with a progressive scarcity of the fine-grained turbidite sequences, expresses the vanishing of the BIS and the progressive retreat of the fluvial systems on the shelf.

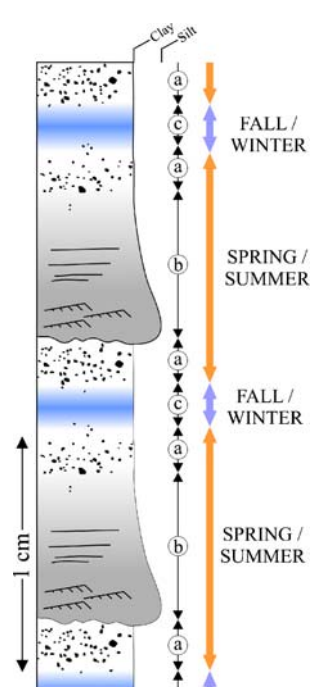


Fig. 9 Conceptual model of a typical meltwater-induced fine-grained turbidite sequence. The unitary sequence is composed of two millimetric IRD-rich layers (**a**) and a fine-grained turbidite deposit (**b**); **c** corresponds to millimetric hemipelagic clay intervals

The transition to lithozone 1 occurs during the Early Holocene (between 10,000 and 8,700 years ^{14}C b.p.). Lithozone 1, characterized by the shutdown of overflow processes on the levees and the occurrence of hemipelagic sedimentation, indicates the establishment of present-day hydrodynamic conditions on the shelf. During the Late Holocene, the cessation of terrigenous supply coincides with the marine invasion of the ‘Fleuve Manche’ palaeoriver (Bourillet et al. 2003), and could also be linked to the general reforestation of Western Europe.

Conclusions

The multi-proxy analysis of long cores on the Whittard, Shamrock and Guilcher turbidite levees highlights the direct influence of the decay of the BIS on the Bay of Biscay deep-sea clastic sedimentation. The chronological framework provides accurate observations on the ‘Fleuve Manche’ and BIS recent histories. The annual BIS cycle of meltwater during the European deglaciation event (15,000 and 14,200 years ^{14}C b.p.) generated seasonal turbidite flows associated with exceptional sedimentation rates in all Celtic and Armorican turbidite systems. Thin-section analysis revealed annual meltwater-induced turbidite sequences consisting of IRD layers each split into two by a fine-grained turbidite. The synchronicity between annual turbidite flow and iceberg release indicates a very short sedimentary transit on the shelf. The annual turbidite/IRD cycles suggest a direct and efficient connection between the ‘Fleuve Manche’ palaeoriver, the Irish Sea continental systems and the submarine canyons. The progressive scarcity of the fine-grained turbidite sequences, associated with the vanishing of ice rafted deposits during the Bølling-Allerød, reflects the collapse of the British-Irish Ice Sheet and the progressive retreat of the fluvial systems on the shelf. Overflow processes on the levees ceased in the Early Holocene (10,000 and 8,700 years b.p.). Since then, hemipelagic sedimentation indicates modern hydrologic conditions on the shelf and the disappearance of the ‘Fleuve Manche’ palaeoriver.

Acknowledgements The authors are grateful to IPEV and the crew of the RV *Marion Dufresne II* for their technical assistance during the SEDICAR and ALIENOR cruises. We wish to thank Y. Balut for his assistance at sea and J. Duprat, G. Floch, B. Martin, J. St. Paul, D. Poirier, R. Kerbrat and O. Ther for their laboratory assistance. Thanks are due to W. Banks and W. Fletcher for assistance with language. We also thank L. Droz and M. Frenz for their very constructive reviews and comments. We acknowledge financial support by the EU project PALEOSTUDIES (contract no. HPRI-CT-2001-0124), the French Programme ‘GDR Marges’ and the ARTEMIS ^{14}C Accelerator Mass Spectrometry French Project. This is U.M.R./EPOC 5805 (Université Bordeaux I-C.N.R.S.) contribution no. 1607.

References

- Auffret GA, Zaragosi S, Voisset M, Droz L, Loubrieu B, Pelleau P, Savoie B, Bourillet J-F, Baltzer A, Bourquin S, Dennielou B, Coutelle A, Weber N, Floch G (2000) Premières observations sur la morphologie et les processus sédimentaires récents de l’Eventail celtique. *Océanol Acta* 23(1):109–116
- Bard E (1998) Geochemical and geophysical implications of the radiocarbon calibration. *Geochim Cosmochim Acta* 62:2025–2038
- Bénard Y (1996) Les techniques de fabrication des lames minces de sol. *Cah Tech INRA* 37:29–42
- Bouma AH (1962) Sedimentology of some flysch deposits: a graphic approach to facies interpretation. Elsevier, Amsterdam
- Bourillet J-F, Lericolais G (2003) Morphology and seismic stratigraphy of the Manche paleoriver system, Western Approaches margin. In: Mienert J, Weaver PP (eds) European Margin sediment dynamics: side-scan sonar and seismic images. Springer, Berlin Heidelberg New York, pp 229–232
- Bourillet J-F, Loubrieu B (1995) Carte bathymorphologique de la marge des entrées de la Manche au 1:250.000. IFREMER, Plouzané
- Bourillet J-F, Turon J-L (2003) Rapport scientifique de la mission MD133/SEDICAR. OCE/2003/04. Les Rapports de Campagne à la Mer, IPEV, Brest
- Bourillet J-F, Reynaud J-Y, Baltzer A, Zaragosi S (2003) The “Fleuve Manche”: the sub-marine formation from the outer shelf to the deep-sea fans. *J Quat Sci* 18:261–282
- Bowen DQ, Phillips FM, McCabe AM, Knutz PC, Sykes GA (2002) New data for the last glacial maximum in Great Britain and Ireland. *Quat Sci Rev* 21(1/3):89–101
- Crémer M, Orsolini P, Ravenne C (1985) Cap-Ferret Fan, Atlantic Ocean. In: Bouma AH, Normark WR, Barnes NE (eds) Submarine fans and related turbidite systems. Springer, Berlin Heidelberg New York, pp 113–120
- Droz L, Auffret GA, Savoie B, Bourillet JF (1999) L’eventail profond de la marge Celtique: stratigraphie et évolution sédimentaire. *C R Acad Sci Paris* 328:173–180
- Faugères JC, Imbert P, Mézerais ML, Crémer M (1998) Seismic patterns of a muddy contourite fan (Vema Channel, South Brazilian Basin) and a sandy distal turbidite deep-sea-fan (Cap Ferret system, Bay of Biscay): a comparison. *Sediment Geol* 115:81–110
- Gibbard PL (1988) The history of great northwest European rivers during the past three millions years. *Philos Trans R Soc Lond B* 318:59–602
- Grousset F, Pujol C, Labeyrie L, Auffret GA, Boelaert A (2000) Were the North Atlantic Heinrich events triggered by the behavior of the European ice sheet? *Geology* 28(2):123–126
- Jensen JHF, Van der Gaast SJ, Koster B, Vaars AJ (1998) CORTEX, a shipboard XRF-scanner for element analyses in split sediment cores. *Mar Geol* 151:143–153
- Lambeck K (1995) Late Devensian and Holocene shorelines of the British Isles and North Sea from models of glacio-hydro-isostatic rebound. *J Geol Soc* 152:437–448
- Larsonneur C, Auffret JP, Smith AJ (1982) Carte des paléo-vallées et des bancs de la Manche orientale (1/50 000). BRGM, Brest
- Lekens WAH, Sejrup HP, Haflidason H, Petersen GO, Hjelstuen B, Knorr G (2005) Laminated sediments preceding Heinrich event 1 in the Northern North Sea and Southern Norwegian Sea: origin, processes and regional linkage. *Mar Geol* 216(1/2):27–50
- Lericolais G, Auffret J-P, Bourillet J-F (2003) The Quaternary Channel River: seismic stratigraphy of its palaeo-valleys and deeps. *J Quat Sci* 18(3/4):245–260

- Le Suavé R (2000) Synthèse bathymétrique et imagerie acoustique. Zone économique exclusive (ZEE). Atlantique Nord-Est, IFREMER, Brest
- Manley PL, Pirmez C, Busch W, Cramp A (1997) Grain-size characterization of Amazon fan deposits and comparison to seismic facies units. In: Flood RD, Piper DJW, Klaus A, Peterson LC (eds) Proc Ocean Drilling Program, Scientific Results, pp 35–52
- Martin GB, Thorrold SR, Jones CM (2004) Temperature and salinity effects on Sr incorporation in otoliths of larval spot (*Leiostomus xanthurus*). Can J Fish Aquat Sci 61:34–42
- McCabe M, Clark PU (1998) Ice sheet variability around the North Atlantic Ocean during the last deglaciation. Nature 392:373–377
- Migeon S, Weber O, Faugères JC, Saint-Paul J (1999) SCOPIX: a new imaging system for core analysis. Geo-Mar Lett 18:251–255
- Mojtahid M, Eynaud F, Zaragosi S, Scourse J, Bourillet J-F, Garlan T (2005) Palaeoclimatology and palaeohydrography of the glacial stages on Celtic and Armorican margins over the last 360,000 yrs. Mar Geol 224(1/4):57–82
- Reynaud JY, Tessier B, Proust JN, Dalrymple R, Marsset T, DeBatist M, Bourillet JF, Lericolais G (1999) Eustatic and hydrodynamic controls on the architecture of a deep shelf sand bank (Celtic Sea). Sedimentology 46(4):703–721
- Richter TO, Lassen S, van Weering TCE, de Haas H (2001) Magnetic susceptibility patterns and provenance of ice-rafterd material at Feni Drift, Rockall Trough: implications for the history of the British-Irish ice sheet. Mar Geol 173(1/4):37–54
- Scourse JD, Hall IR, McCave IN, Young JR, Sugdon C (2000) The origin of Heinrich layers: evidence from H₂ for European precursor events. Earth Planet Sci Lett 182(2):187–195
- Skene KI, Piper DJW, Hill PS (2002) Quantitative analysis of variations in depositional sequence thickness from submarine channel levees. Sedimentology 49:1411–1430
- Turon JL, Bourillet J-F, Equipe ALIENOR (2004) Résultats préliminaires de la mission ALIENOR-MD141-Partie 2. IPEV, Brest
- Zaragosi S, Auffret GA, Faugères JC, Garlan T, Pujol C, Cortijo E (2000) Physiography and recent sediment distribution of the Celtic Deep-sea Fan, Bay of Biscay. Mar Geol 169:207–237
- Zaragosi S, Eynaud F, Pujol C, Auffret GA, Turon J-L, Garlan T (2001a) Initiation of the European deglaciation as recorded in the northwestern Bay of Biscay slope environments (Meriadzek Terrace and Trevelyan Escarpment): a multi-proxy approach. Earth Planet Sci Lett 188(3/4):493–507
- Zaragosi S, Le Suave R, Bourillet J-F, Auffret GA, Faugères J-C, Pujol C, Garlan T (2001b) The deep-sea Armorican depositional system (Bay of Biscay), a multiple source, ramp model. Geo-Mar Lett 20(4):219–232